Polyoxometalate-Based Complex with Visible-Light Photochromism as Electrocatalyst for Generating Hydrogen from Water

Yun Gong, [*,a] Yong Xi Yang, [a] Miao Miao Zhang, [a] Xiao Lin Gao, [a]Jun Li Yin [a] and Jian Hua Lin[*,a,b]

[a]*Department of Applied Chemistry, College of Chemistry and Chemical Engineering, Chongqing University, Chongqing 400030, P. R. China Tel: +86-023-65106150*

E-mail: gongyun7211@cqu.edu.cn

[b]*Zhejiang University, Hangzhou 310058, P. R. China Tel: +86-0571-88981583*

E-mail: jhlin@cqu.edu.cn; jhlin@zju.edu.cn; jhlin@pku.edu.cn

Determination of Faradaic Efficiency

Controlled potential electrolyses were conducted in a 50 mL 0.5 M Na_2SO_4 solution at an applied potential of □-1.4 V vs SCE (η = -0.76 V) for 0.5 hour. The pH change of the solution during the electrolysis was recorded with a pH meter. Assuming 100% Faradaic efficiency, the theoretical pH change over time can be calculated by the equation of pH = 14 + lg {Σ(It)/(FV)}, where I = current (A), t = time (s), F = Faraday constant (96485 C/mol), V = solution volume (0.05 L). [1] The amount of H_2 evolved was determined using gas chromatography (GC, 7890A, thermal conductivity detector (TCD), Ar carrier, Agilent). The theoretical (assuming 100% Faradic efficiency) hydrogen volume is based on the amount of consumed charge during the course of electrolysis.

Table S1 Selected bond lengths (Å) and angles (º) for complexes **1** and **2**

Complex 1			
Mo(1)-O(5)	1.697(5)	Mo(1)-O(2)	2.431(4)
Mo(2)-O(7)	1.701(5)	Mo(2)-O(1)	2.315(5)
Mo(3)-N(1)	2.243(6)	Mo(3)-O(11)	1.684(6)
Mo(3)-O(1)	2.317(5)	Mo(4)-O(2)#1	2.227(5)
Mo(4)-O(12)	1.700(6)	Mo(4)-O(4)#1	2.382(5)
O(2)#1-Mo(1)-O(3)	73.46(18)	O(5)-Mo(1)-O(2)	179.2(2)
O(8)-Mo(2)-O(2)	72.93(18)	O(9)-Mo(2)-O(1)	165.3(2)
O(3)-Mo(3)-O(1)	69.63(17)	O(11)-Mo(3)-O(1)	167.3(2)
O(3)-Mo(3)-N(1)	79.18(19)	O(6)-Mo(3)-N(1)	160.9(2)
Complex 2			
Co(1)-N(8)	1.946(9)	Co(1)-N(6)	1.980(9)
Co(1)-N(1)	1.953(9)	Co(1)-N(13)	1.977(8)
O(4)-P(1)	1.513(6)	O(1)-P(1)	1.554(6)
Mo(3)-O(12)	1.693(7)	Mo(4)-O(4)#2	2.368(6)
N(1)-Co(1)-N(6)	81.2(4)	N(13)-Co(1)-N(6)	178.7(4)
N(1)-Co(1)-N(13)	98.5(4)	N(8)-Co(1)-N(1)	177.4(4)
N(8)-Co(1)-N(13)	81.4(4)	N(8)-Co(1)-N(6)	98.9(4)
O(5)-Mo(2)-O(3)#2	70.4(3)	O(7)-Mo(4)-O(7)#3	173.8(4)
O(2)-P(1)-O(3)	108.1(4)	O(4)-P(1)-O(2)	111.7(4)

Symmetry transformations used to generate equivalent atoms:

#1 -x+3/2, -y+1/2, -z+1 #2 -x+1, y, -z+3/2 #3 -x+2, y, -z+3/2

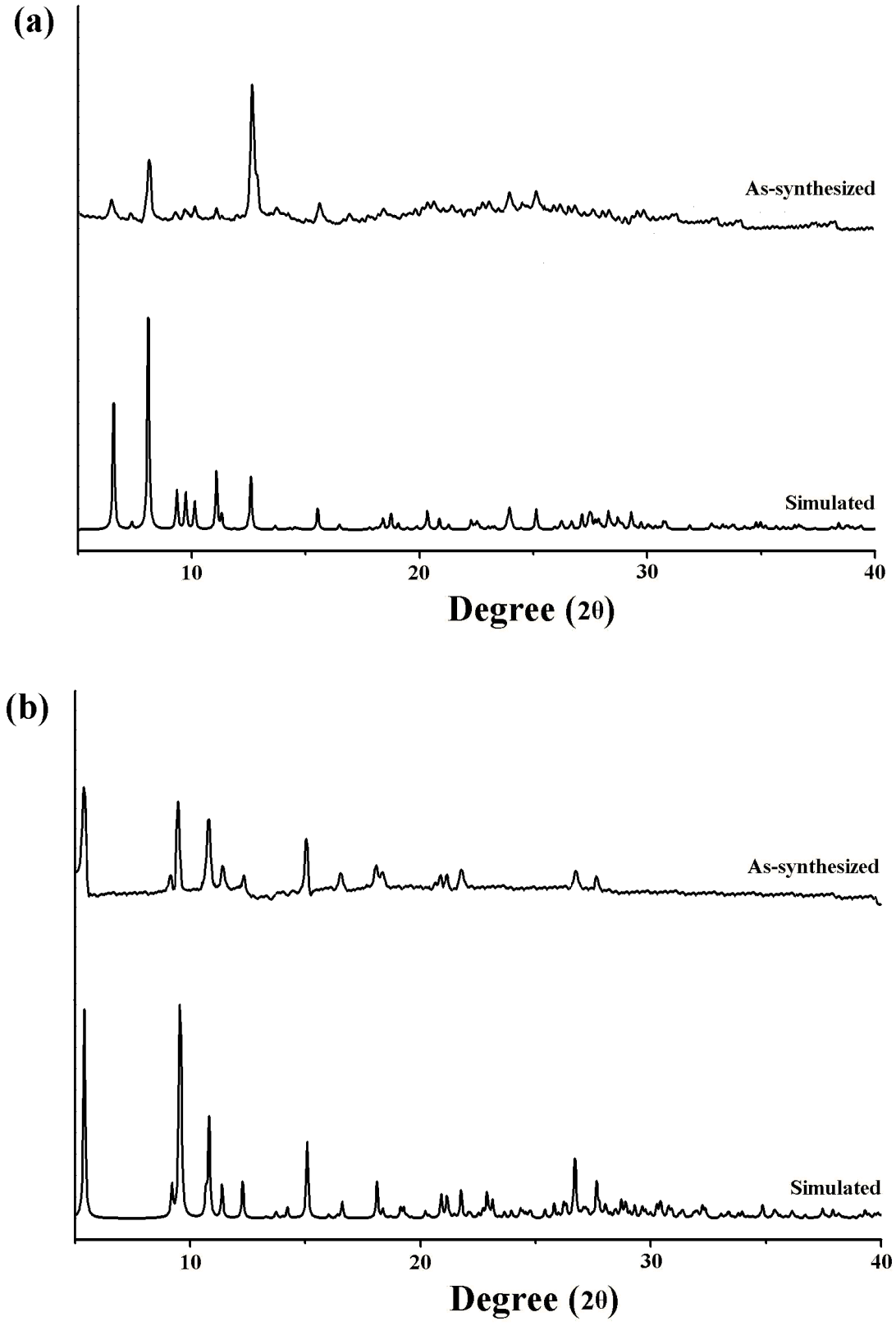

Fig. S1 The powder XRD patterns for complexes **1** (**a**) and **2** (**b**).

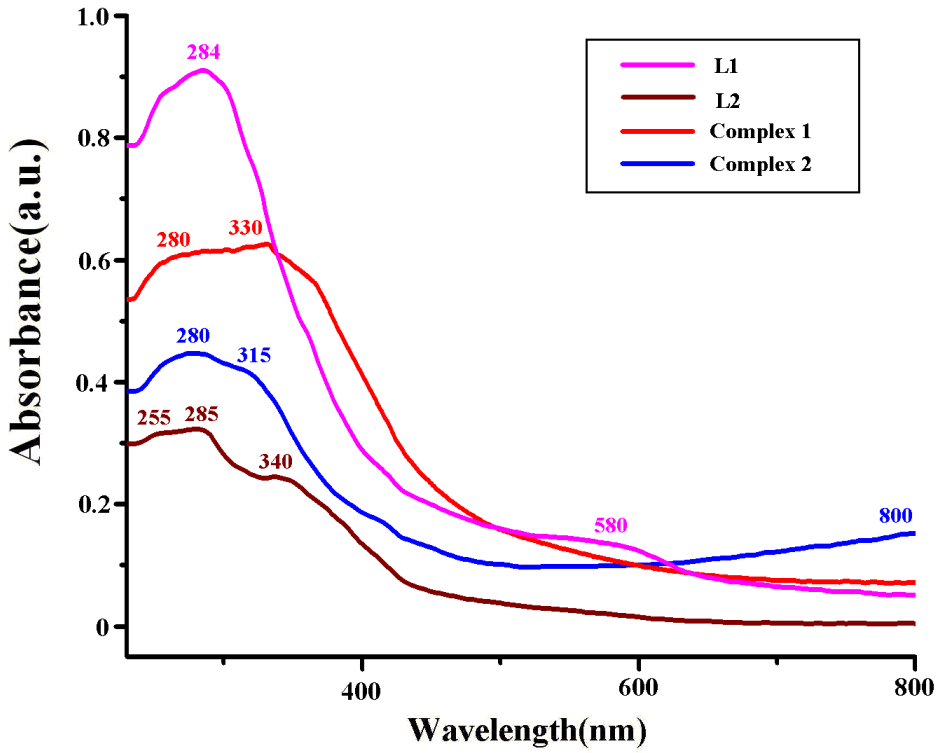

Fig. S2 UV-vis absorption spectra at room temperature for the free organic ligands and complexes **1**-**2** in the solid state.

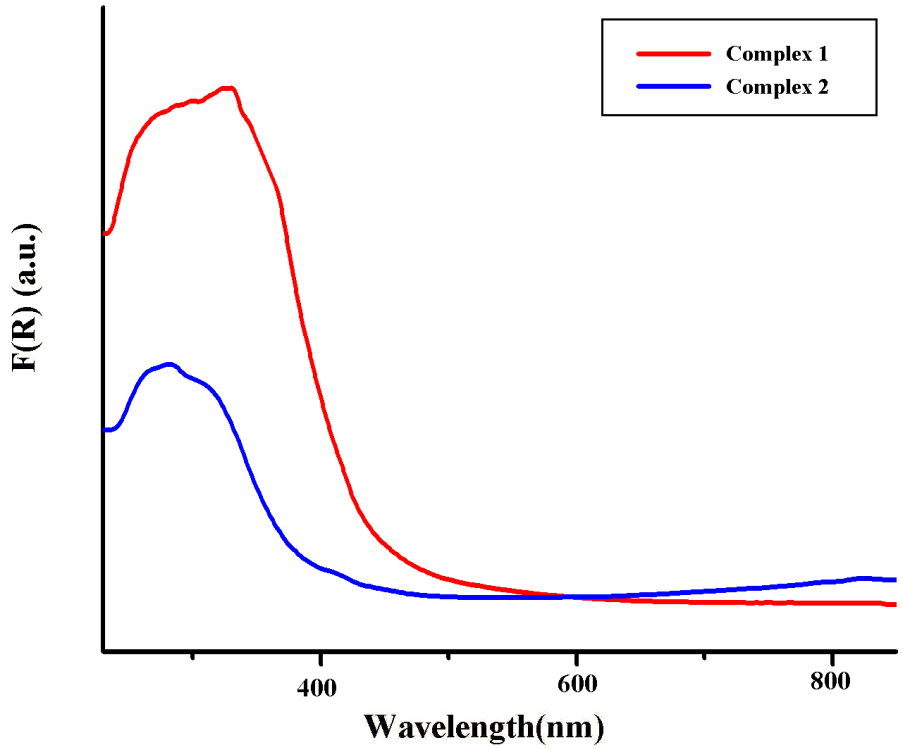

Fig. S3 The diffuse reflectance spectra of complex **1** and **2** in Kubelka–Munk units. F(R) is the Kubelka–Munk function, where $F(R) = (1-R)^2/2R$, R is the experimentally observed reflectance.

The formula for the calculation of band gap is as follows:

Band Gap energy = $hc/\lambda = 1240/\lambda$ eV

h = planks constant = 6.626×10^{-34} Joules ·sec

c = Speed of light = 3.0×10^{8} meter/sec

λ = cut off wavelength (nm)

where 1eV = 1.6×10^{-19} Joules (conversion factor)

λ, the cut off wavelength, is obtained according to the diffuse reflectance spectrum {F(R) vs. wavelength, $F(R) = (1-R)^2/2R$, R is the experimentally observed reflectance}.

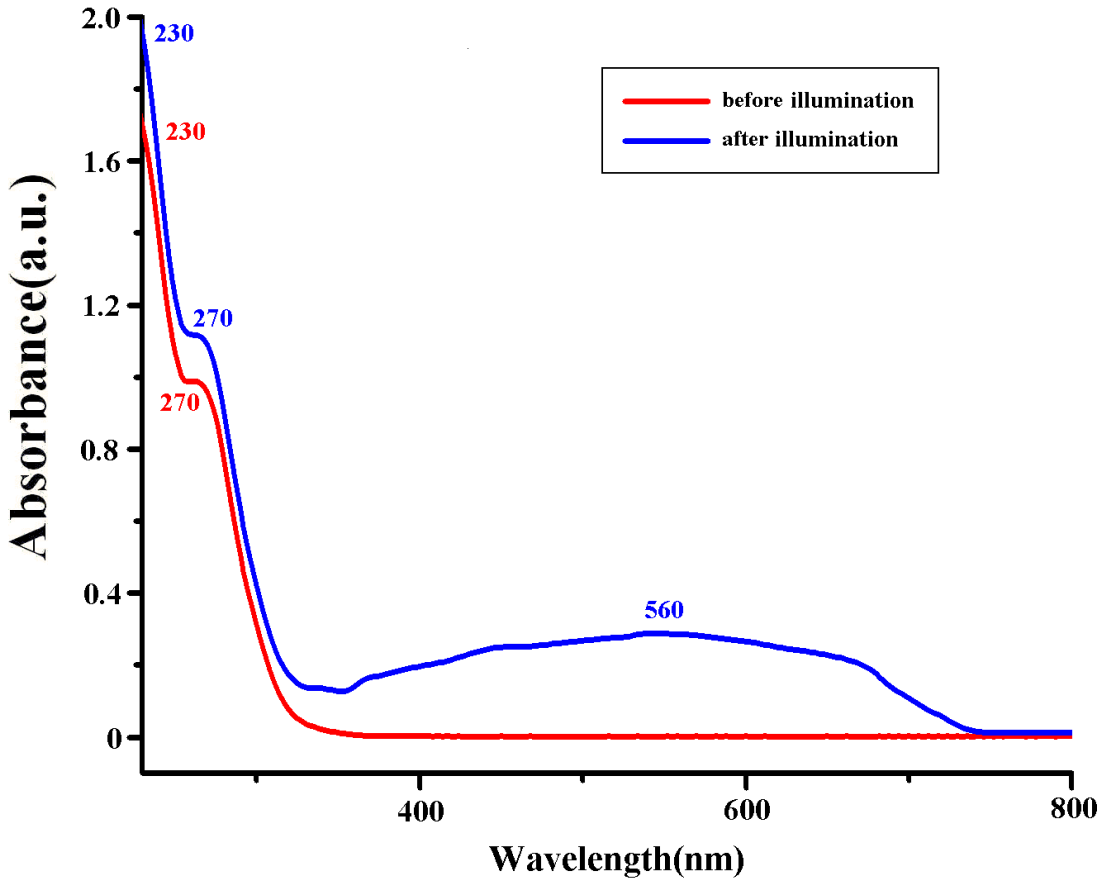

Fig. S4 UV-vis absorption spectra at room temperature for the Na_2SO_4 solution of complex **1** before and after visible-light illumination ($\lambda > 400$ nm).

(a)

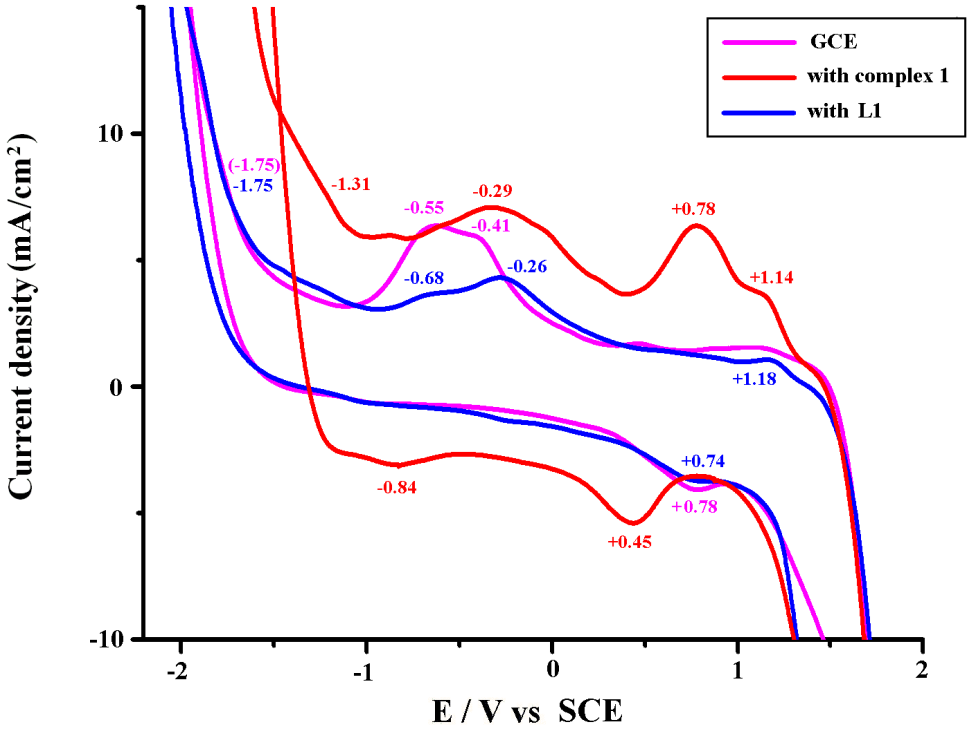
GCE
with complex 1
with L1
Current density (mA/cm²)
E / V vs SCE
(-1.75)
-1.75
-1.31
-0.55
-0.29
-0.41
-0.68
-0.26
+0.78
+1.14
+1.18
+0.74
+0.78
-0.84
+0.45

(b)

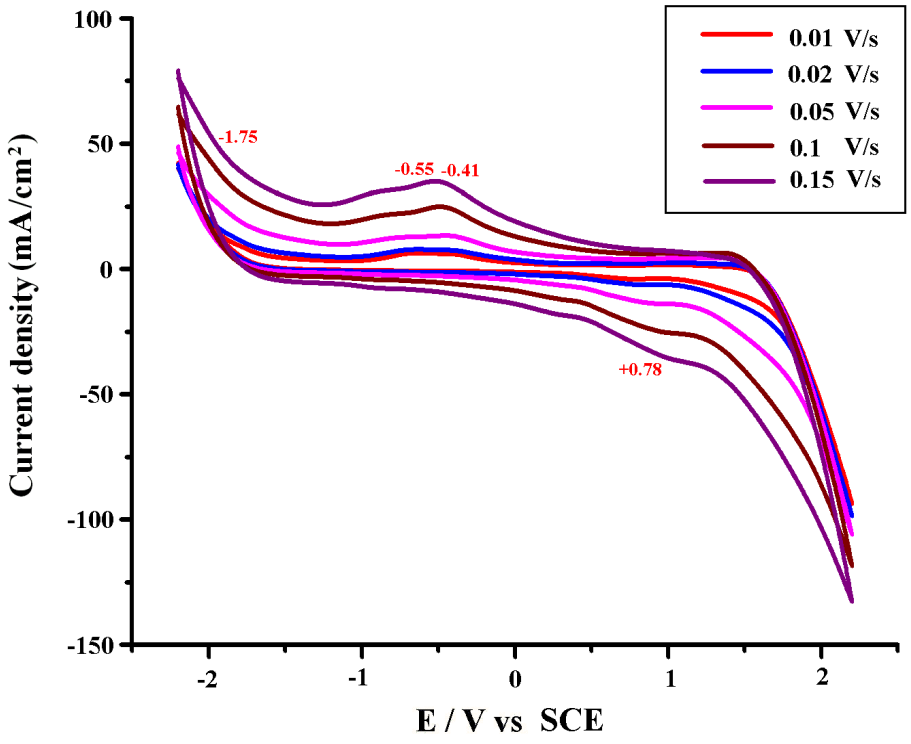
0.01 V/s
0.02 V/s
0.05 V/s
0.1 V/s
0.15 V/s
Current density (mA/cm²)
E / V vs SCE
-1.75
-0.55
-0.41
+0.78

Fig. S5 CVs of the bare GCE in the 0.5 M Na_2SO_4 aqueous solution (40 mL) at a scan rate of 0.01 $V \cdot s^{-1}$ in the absence (pink) and presence of 4 mg L1 (blue) or 4 mg complex **1** (red) (**a**); CVs of the GCE in the 0.5 M Na_2SO_4 solution (40 mL) at different sweep rates (**b**).

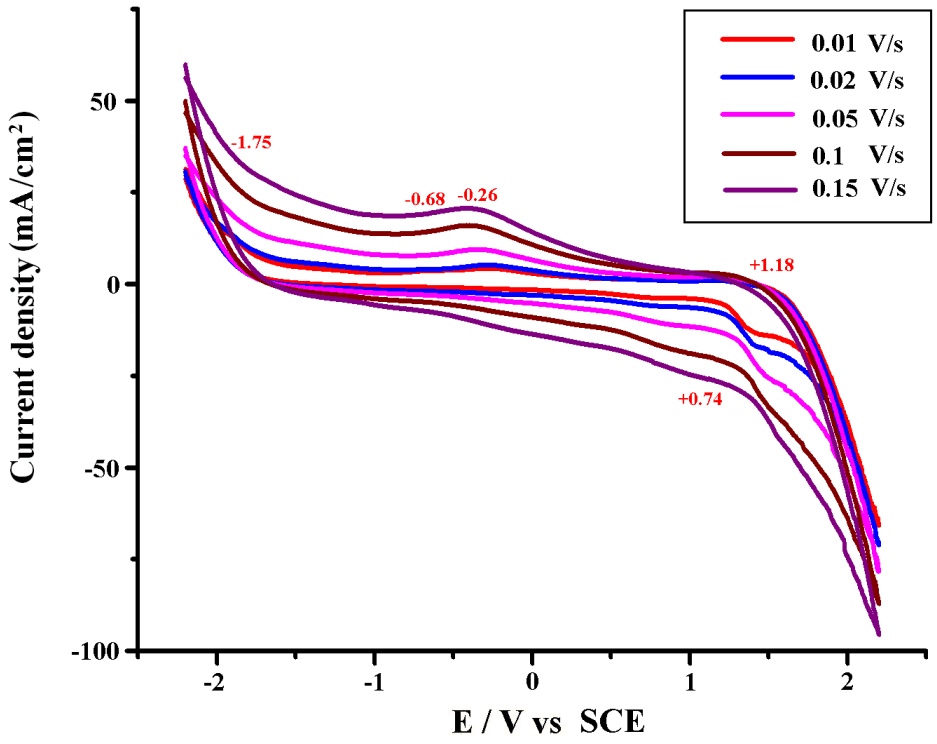

Fig. S6 CVs of the GCE in 0.5 M Na_2SO_4 solution (40 mL) in the presence of 4 mg L1 at different sweep rates.

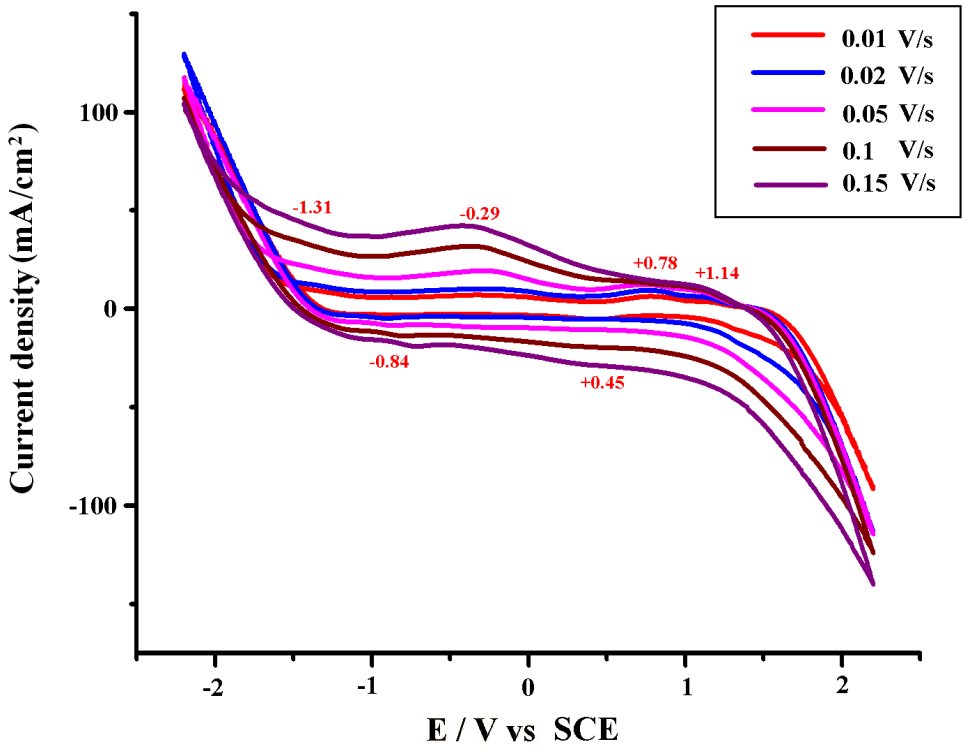

Fig. S7 CVs of the GCE in 0.5 M Na_2SO_4 solution (40 mL) in the presence of 4 mg complex **1** at different sweep rates.

.

(**a**)

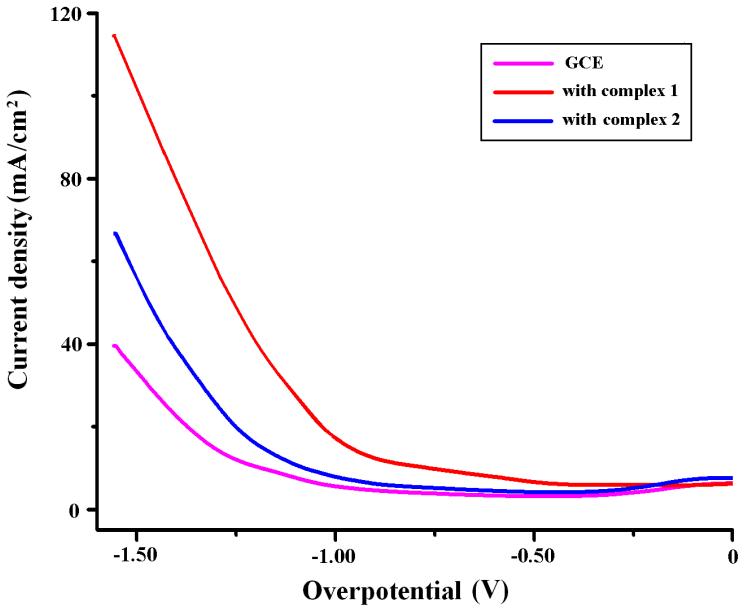

(**b**)

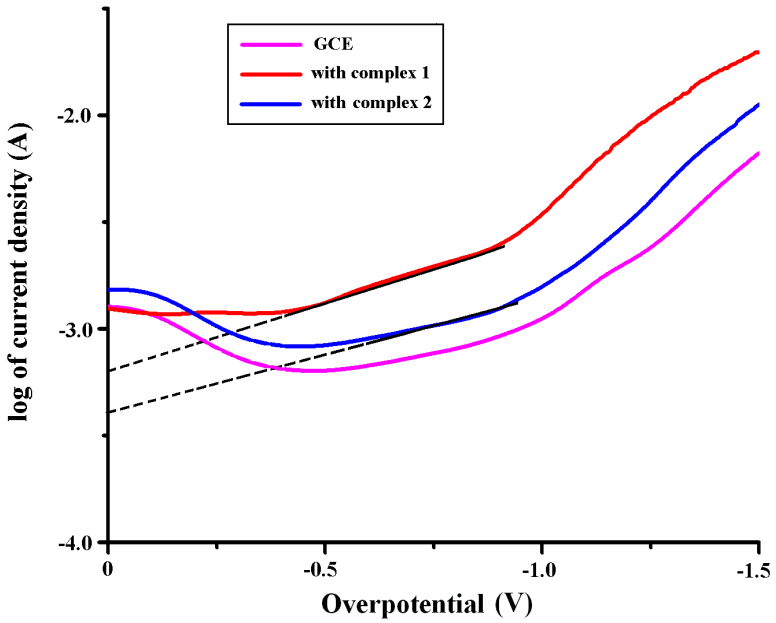

Fig. S8 Current intensity (*i*) / overpotential (η) diagrams (**a**) for the HER at the bare GCE in the absence and presence of 4 mg complex **1** or **2** in 0.5 M Na_2SO_4 solution (40 mL) at sweep rates of 0.01 $V \cdot s^{-1}$; Tafel plots of *logi* against overpotential η for the HER (The

linear part of the Tafel curves denoted in black dotted lines with the intercept at the *y* axis) (**b**).

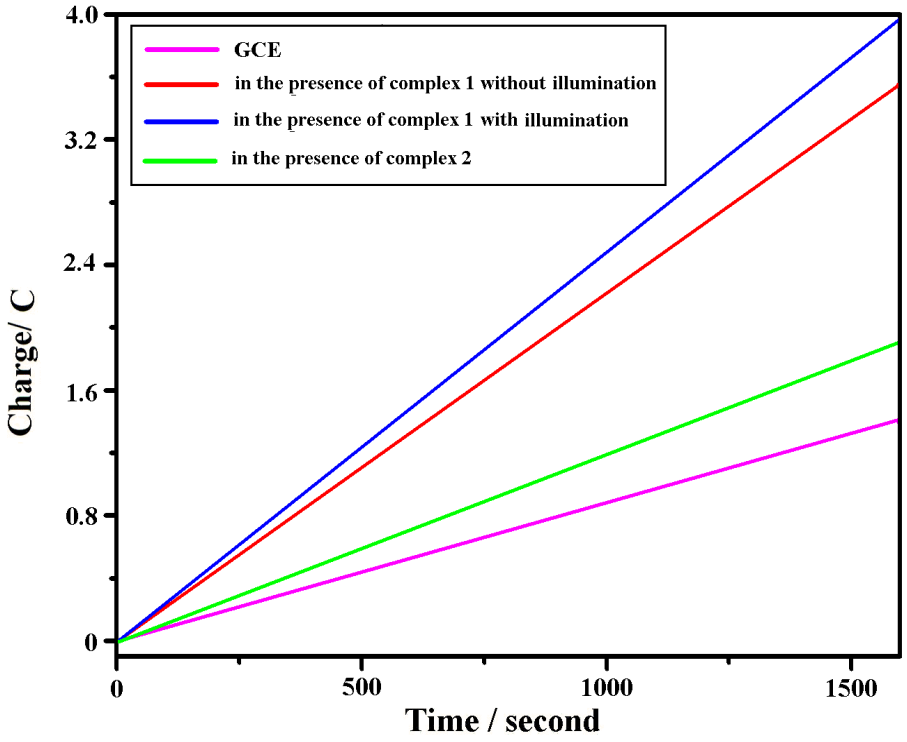

Fig. S9 Controlled potential electrolysis of the bare GCE in the 0.5 M Na_2SO_4 aqueous solution (40 mL) in the absence (current density = 4.0 mA/cm^2) (pink) and presence of complex **1** with (red) or without visible-light illumination (current density = 9.9 mA/cm^2) (blue) or in the presence of complex **2** (current density = 5.2 mA/cm^2) (green), showing charge buildup versus time with an applied potential of -1.4 V vs SCE (η = -0.76 V).

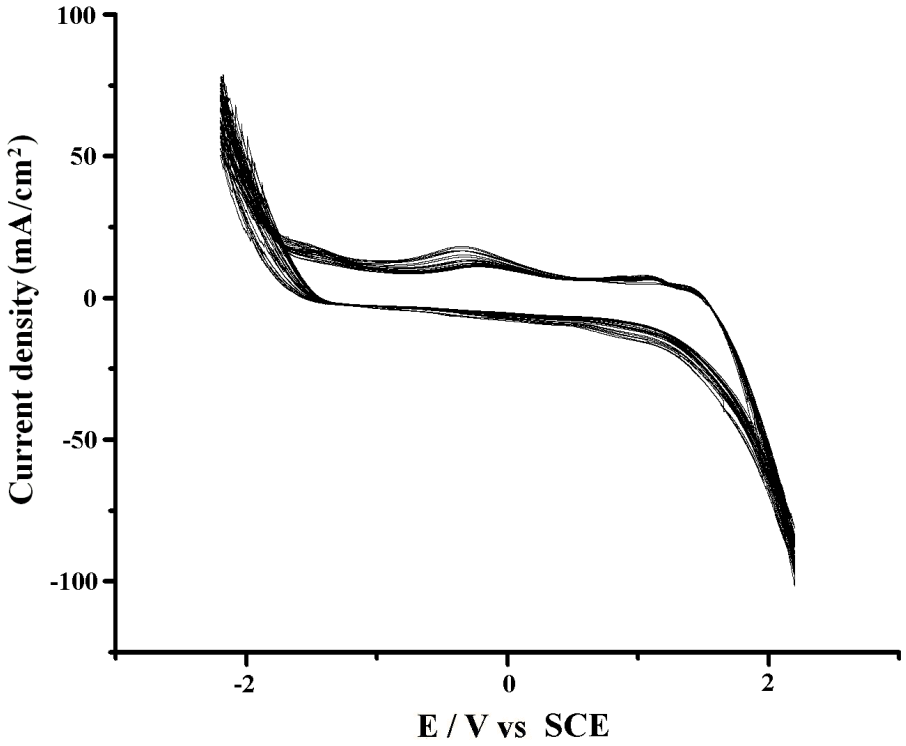

Fig. S10 Dozens of CVs of the bare GCE in the 0.5 M Na_2SO_4 aqueous solution (40 mL) at a scan rate of 0.05 $V \cdot s^{-1}$ in the presence of 4 mg complex **1**.

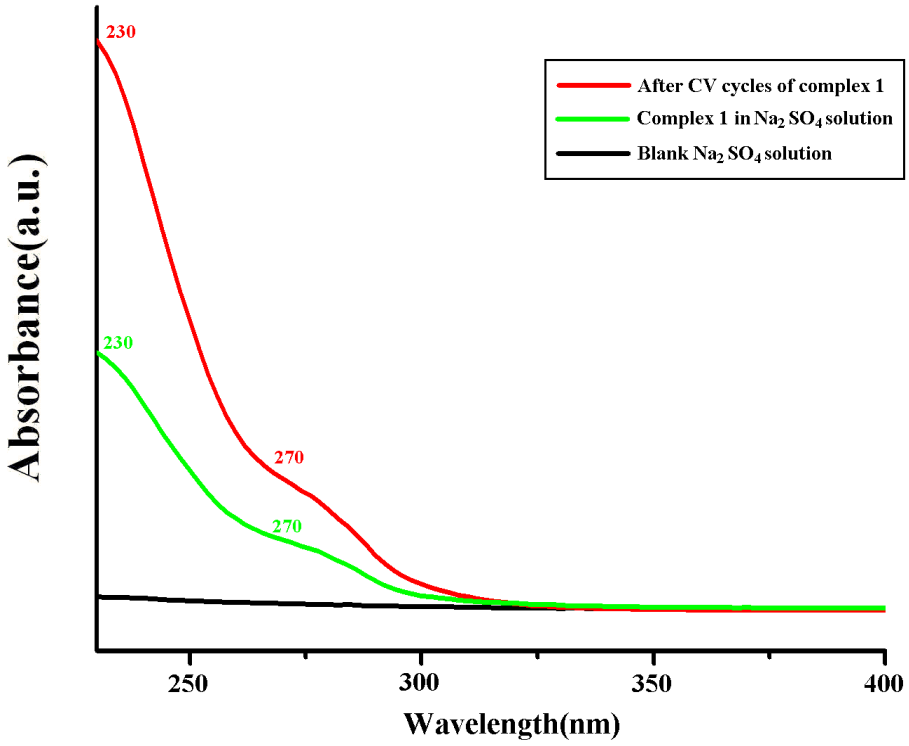

Fig. S11 UV absorption spectra at room temperature for the blank Na_2SO_4 solution (black), the Na_2SO_4 solution of complex **1** (green) and the solution of complex **1** after CV cycles (red).

(a)

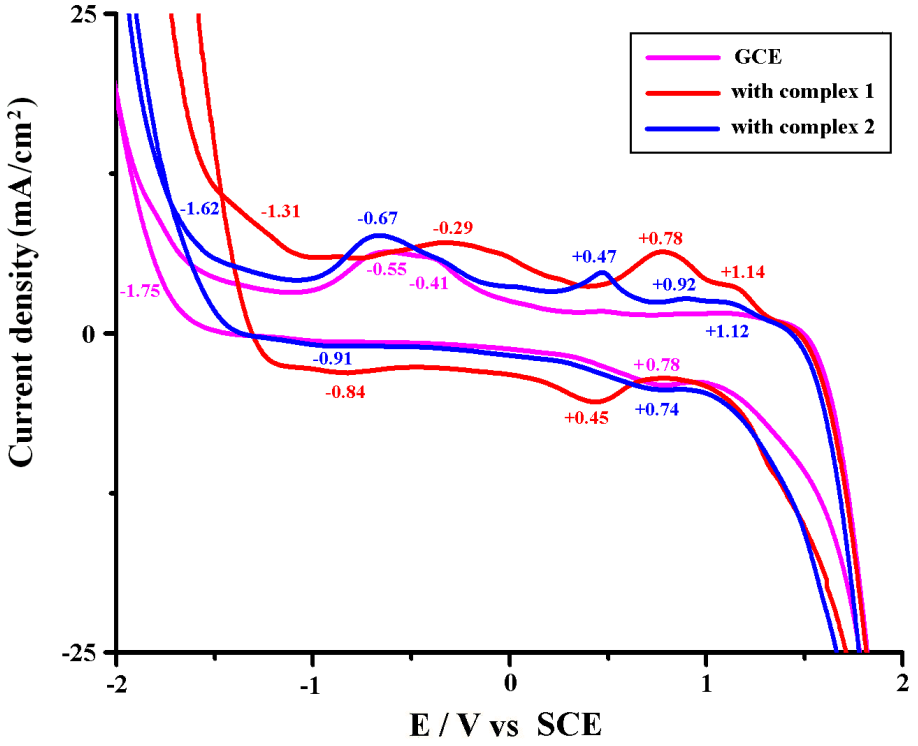
GCE
with complex 1
with complex 2
Current density (mA/cm²)
E / V vs SCE
25
0
-25
-2
-1
0
1
2
-1.75
-1.62
-1.31
-0.67
-0.29
-0.55
-0.41
+0.47
+0.78
+0.92
+1.14
+1.12
-0.91
-0.84
+0.78
+0.45
+0.74

(b)

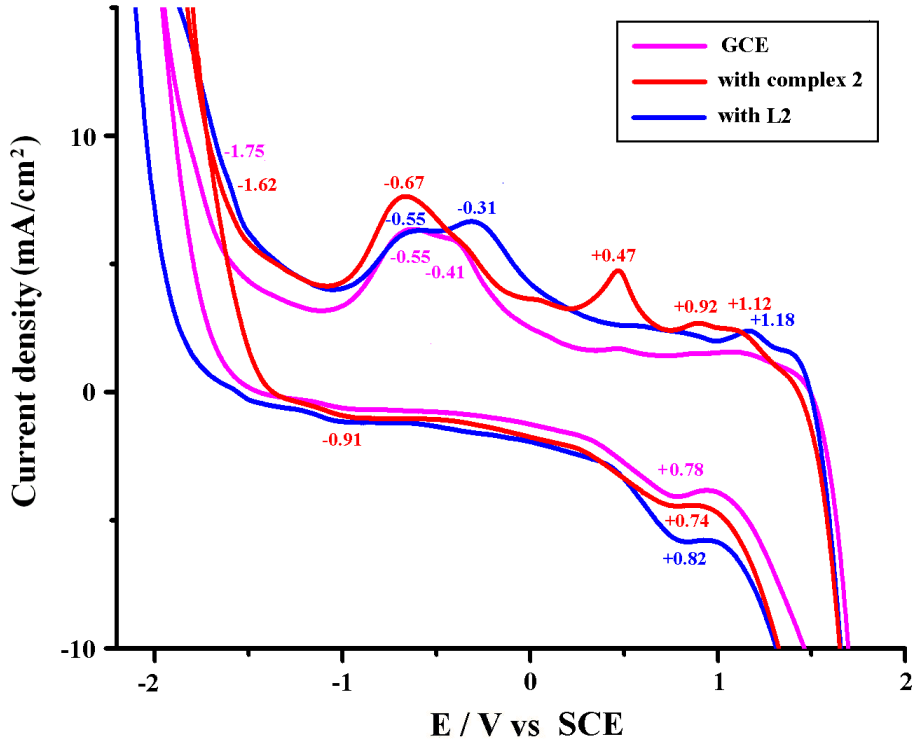
GCE
with complex 2
with L2
Current density (mA/cm²)
E / V vs SCE
10
0
-10
-2
-1
0
1
2
-1.75
-1.62
-0.67
-0.55
-0.31
-0.55
-0.41
+0.47
+0.92
+1.12
+1.18
-0.91
+0.78
+0.74
+0.82

Fig. S12 CVs of the bare GCE in the 0.5 M Na_2SO_4 aqueous solution (40 mL) at a scan rate of 0.01 $V \cdot s^{-1}$ in the absence (pink) and presence of 4 mg complex **1** (red) or complex **2** (blue) (**a**); CVs of the bare GCE in the 0.5 M Na_2SO_4 aqueous solution (40 mL) at a scan rate of 0.01 $V \cdot s^{-1}$ in the absence (pink) and presence of 4 mg L2 (blue) or 4 mg complex **1** (red) (**b**).

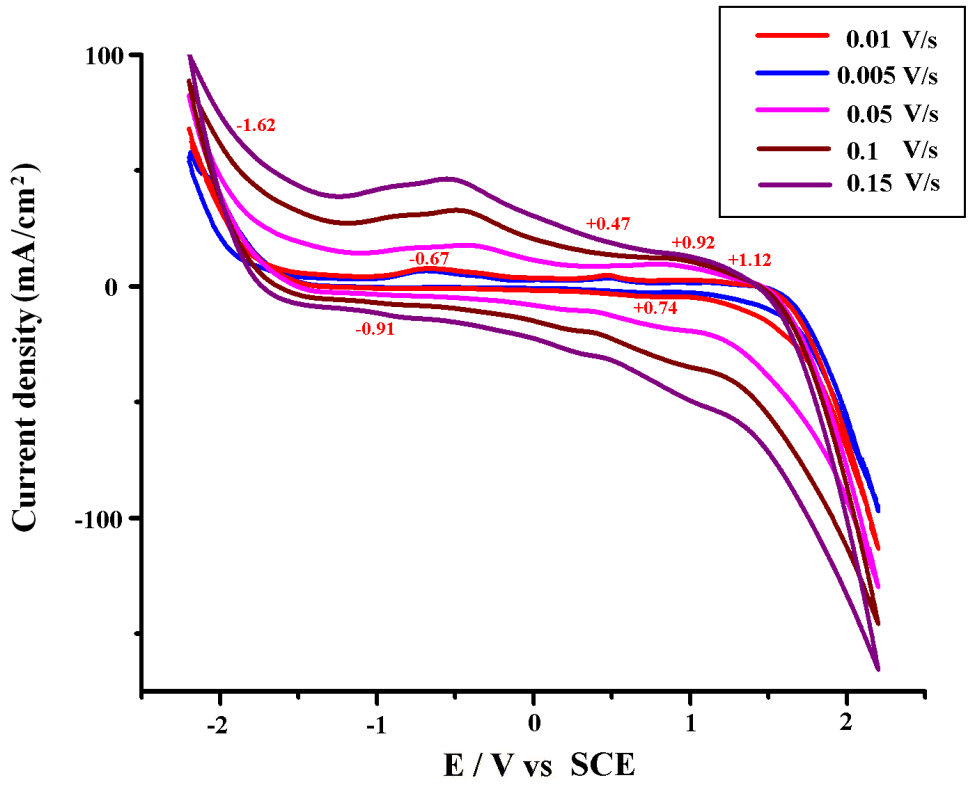

Fig. S13 CVs of the GCE in 0.5 M Na_2SO_4 solution (40 mL) in the presence of 4 mg complex **2** at different sweep rates.

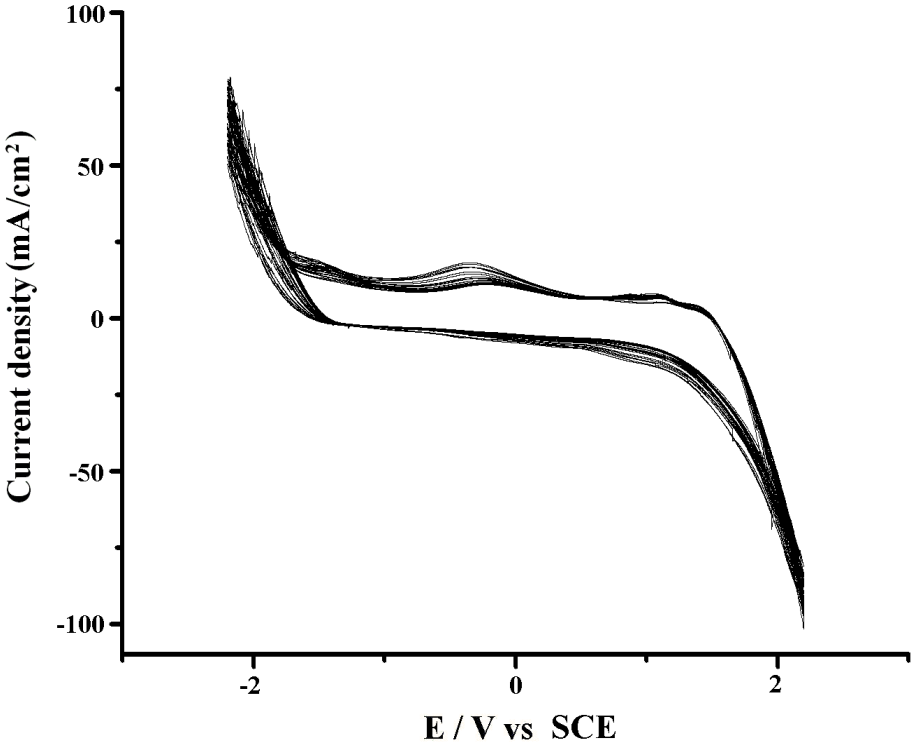

Fig. S14 Dozens of CVs of the bare GCE in the 0.5 M Na_2SO_4 aqueous solution (40 mL) at a scan rate of 0.05 $V \cdot s^{-1}$ in the presence of 4 mg complex **2**.

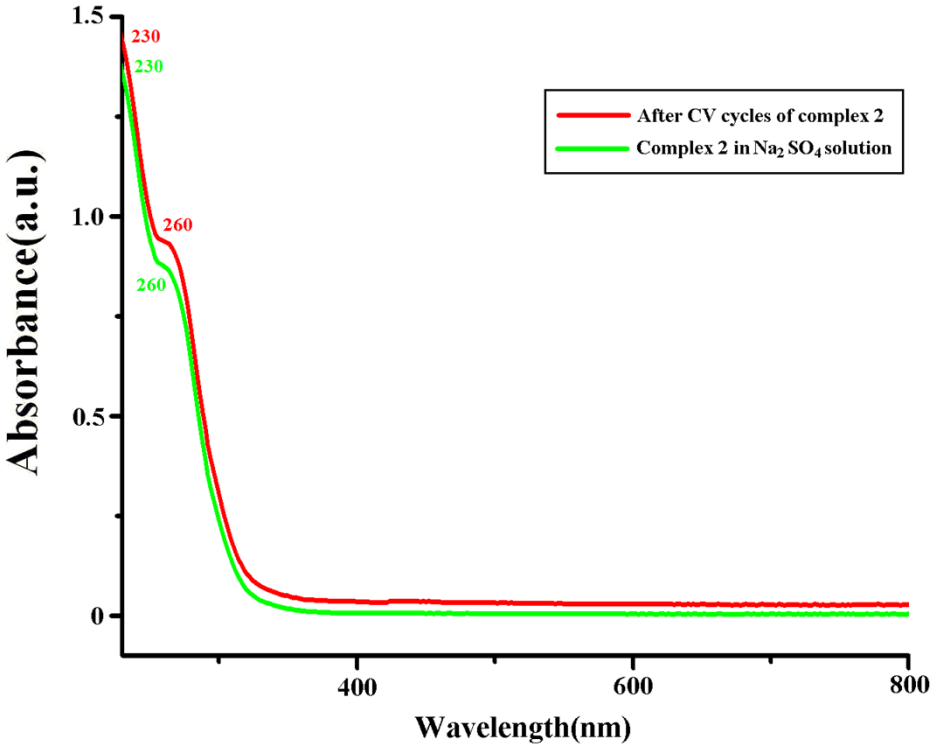

Fig. S15 UV-vis absorption spectra at room temperature for the Na_2SO_4 solution of complex **2** before (green) and after CV cycles (red).

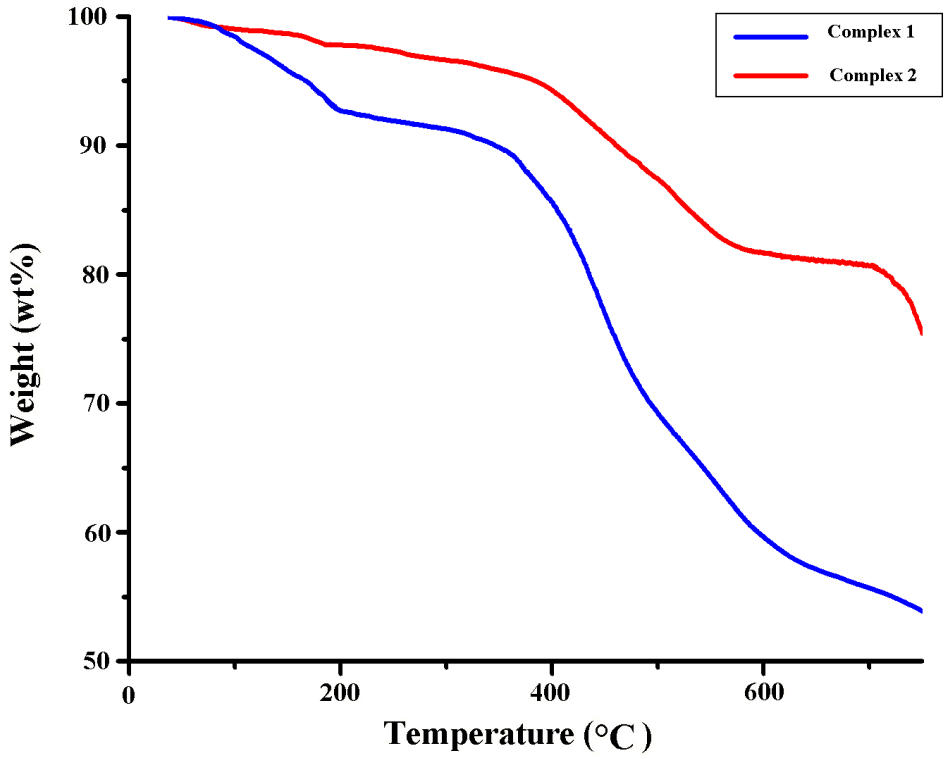

Fig. S16 Thermogravimetric curves of complexes **1** and **2**.

References:

1 Y. J. Sun, J. P. Bigi, N. A. Piro, M. L. Tang, J. R. Long and C. J. Chang, *J. Am. Chem. Soc.*, **2011**, *133*, 9212.